



Effect of coastal waves on sea level in Óbidos Lagoon, Portugal

Madalena S. Malhadas^{a,*}, Paulo C. Leitão^b, Adélio Silva^b, Ramiro Neves^a

^a Instituto Superior Técnico, Departamento de Mecânica, Av. Rovisco Pais, 1049-001 Lisboa, Portugal

^b Hidromod, Modelação em Engenharia, Lda., Av. Manuel da Maia, n.º 36, 3.ª Esq., 1000-201 Lisboa, Portugal

ARTICLE INFO

Article history:

Received 21 May 2008

Received in revised form

28 January 2009

Accepted 2 February 2009

Available online 28 February 2009

Keywords:

MOHID

Hydrodynamic

Wave radiation stresses

Wave set-up

Tidal inlet morphology

Óbidos Lagoon

ABSTRACT

This study reports the role of waves, tide, wind and freshwater discharges over the sea level in Óbidos Lagoon, a coastal system connected to the sea through a narrow and shallow mobile inlet. To address the hydrodynamic features of this coastal system, the relative importance of different physical forcings were evaluated. For this purpose, observations together with realistic and idealized numerical modeling were used. Both model and measurements show that the lagoon sea level remains above offshore sea level during storm wave periods. Hence, a simplified inlet-lagoon idealized model was described through mathematical expressions, to understand and highlight the physical processes responsible for sea-level elevation.

In general, it can be concluded that multiple forcing conditions, specifically tide and waves, are important in defining the dynamics of the Óbidos Lagoon. The variability of the lagoon sea level is 80% due to tide and 20% due to waves. A correlation was found with wave height and sea-level elevation during high wave activity periods; no correlation was found for low wave activity. A significant super-elevation on lagoon sea level occurs during storm wave periods. Such super-elevation is explained, not only by wave set-up or radiation stresses due to waves, but also by tidal inlet morphology (mainly depth and length).

© 2009 Elsevier Ltd. All rights reserved.

1. Introduction

Direct (wind) and indirect atmospheric (rain, through river flow) and marine (tide and waves) forces cause large differences and rapid changes in the physical and the chemical characteristics of coastal lagoons (Troussellier and Gattuso, 2007). These systems are typically shallow, fresher than near-ocean conditions and are separated by sand spits or barrier islands (Fortunato and Oliveira, 2007). The hydrodynamic behavior in these coastal systems is driven mainly by tide and waves. The presence of waves can cause large differences in terms of sea-level variations (Nielsen and Apelt, 2003); their relative importance depends upon the morphology of the lagoon entrance, as well as the local wave regime. In shallow and narrow entrances, the sea-level elevation caused by wave motion, such as wave breaking, is an important mechanism. This rise in sea level, or set-up, induced by waves is commonly termed as “wave set-up” (Angwenyi and Rydberg, 2005). The theoretical background of wave set-up was introduced by Longuet-Higgins and Stewart (1960, 1962, 1964), who related

the effect to the concept of radiation stresses, due to the presence of waves. Basically, the radiation stress is defined as the excess of flow of momentum due to the presence of waves (Longuet-Higgins and Stewart, 1973). This original analysis established a relationship between the gradient of the radiation stresses for waves approaching the beach at an oblique angle, and the resulting of alongshore current (Nielsen and Apelt, 2003).

Factors governing the relative magnitude of wave set-up at tidal inlets and river entrances have been addressed by Guza and Thornton (1981), Hanslow and Nielsen (1992), Hanslow et al. (1996), Dunn et al. (2000), Dunn (2001), Oshiyama et al. (2001), Tanaka et al. (2000, 2003) and Nguyen et al. (2007). In the past Dunn (2001) explained a part of the “missing” or “lack” of set-up in the Brunswick River, Australia. The explanation was based upon the mechanism of wave height decay. Recently, Nguyen et al. (2007) showed that set-up, or sea-level elevation, depends not only upon offshore wave height but also on the different morphological river entrances or tidal inlets. These authors found a correlation between wave set-up height and water depth of the entrance, based upon data collected in seven different morphological river entrances and one inlet. They showed that the wave set-up height is inversely proportional to the average water depth, at a river or inlet entrance.

In most cases, the estimation of wave set-up at entrances was based upon only observations. Numerical models, on the other

* Corresponding author. Tel.: +351 218419432; fax: +351 218419423.

E-mail addresses: madalena.maretec@ist.utl.pt (M.S. Malhadas), paulo.cham-bel@hidromod.com (P.C. Leitão), adelio@hidromod.com (A. Silva), ramiro.neves@ist.utl.pt (R. Neves).

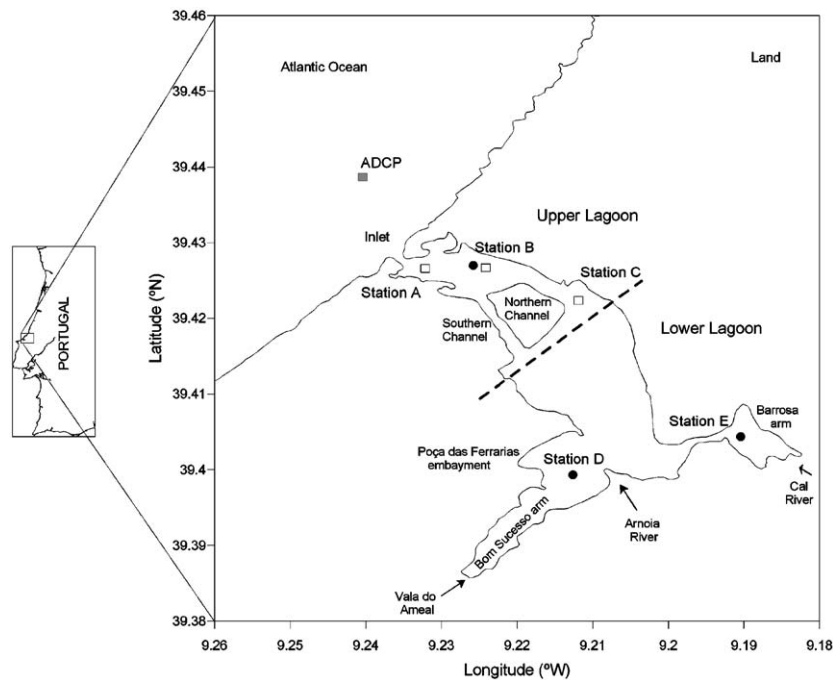


Fig. 1. Geographical location of the Óbidos Lagoon. Tidal gauges (●), current measurement stations (□); and river discharges are represented also in the Figure, as well as the main basins.

hand, provide an approach to the study of the importance of simulating effect of waves or other external forces (e.g., winds) upon the hydrodynamic behavior. In addition, hydrodynamic model applications are useful in understanding the main physical processes, since the complete field data sets is, however, hard to obtain.

The main purpose of this study is to evaluate the dominating driving forces on sea-level rise (SLR) in the Óbidos Lagoon, a coastal system located on the western Portuguese coast (Fig. 1), connected to the sea through a narrow, shallow and mobile inlet. Fluctuations in lagoon sea level (LSL), under distinct physical forcing, are analyzed: (i) tide; (ii) tide and wind; (iii) tide and freshwater river discharges; and (iv) tide and waves. To achieve the main objective, field measurements and numerical modelling were used, in addition to an idealized inlet-lagoon model. Field data are useful to develop an understanding of the hydrodynamic features of the coastal system and numerical model validation. The results show a rise in the LSL, during storm wave periods. This SLR can be attributed not only to wave-induced effects but also to the inlet morphology (depth and length).

This contribution is arranged as follows. Section 2 describes the study area, field sites and measurements obtained in the coastal area and in the lagoon; it introduces also the numerical model. Section 3 presents an analysis of the observations and numerical simulations, together with the inlet-lagoon idealized model. Finally, the major findings are summarized in Section 4.

2. Materials and methods

This analysis combines field data and numerical model predictions. Initially, bathymetric and sea-level data were used as a preliminary assessment, of the morphological and the hydrodynamic characteristics of the lagoon. These data were used then to validate the hydrodynamic numerical model. Subsequently, the hydrodynamic model was used to simulate the LSL, under several physical forcings. The following sub-sections

describe the study area and summarize the characteristics of the field data and the model set-up.

2.1. Description of the system

The Óbidos Lagoon is a small and shallow coastal lagoon with a surface area of 7 km² and 2 m average depth (Vão, 1991). The Óbidos Lagoon consists of two regions, with distinct morphological hydrodynamic characteristics (Fig. 1): the lower and the upper lagoon. The lower lagoon, connected to the Atlantic Ocean, is composed of several channels (Carvalho et al., 2006). The water velocities in this region often exceed 1 ms⁻¹ along the northern channel and about 1.6 ms⁻¹ in the inlet (Malhadas, 2008). The upper lagoon consists of a shallow basin, elongated arms (Barroa and Bom Sucesso) and a small embayment in the south (Poça das Ferrarias, Oliveira et al., 2006). Because the velocities are weaker (0.4 ms⁻¹ in the arms, Malhadas, 2008), sediments originating from various tributaries tend to settle out in this part of the lagoon (Fortunato and Oliveira, 2007). Freshwater inflow enters the lagoon at both arms: the Cal River at the Barroa arm and Vala do Ameal at the Bom Sucesso arm. The Arnóia River discharge, between the lagoon arms, contributes about 90% of freshwater fluxes into the lagoon. The river is the major source of sediments, whose deposition has created an extensive sand bank.

This shallow lagoon is characterized by semi-diurnal tides (tidal range 0.5–4.0 m depending upon location and tidal phase) enabling important water exchanges to take place with the coastal waters. These are estimated at 6×10^6 m³ for an average neap tide and 10^7 m³ for a spring tide (Santos et al., 2006).

Overall, freshwater input plays a minor role, with average flow rates of the order of 3 m³ s⁻¹; this is less than 5% of the average tidal prism, scaled by the M2 period (Rego, 2004). The influence of the tide extends throughout the entire lagoon, without pronounced longitudinal variation in salinity or stratification (Carvalho et al., 2005). Salinity from the upper to the lower lagoon varies from 34 to 36 (Santos et al., 2006).

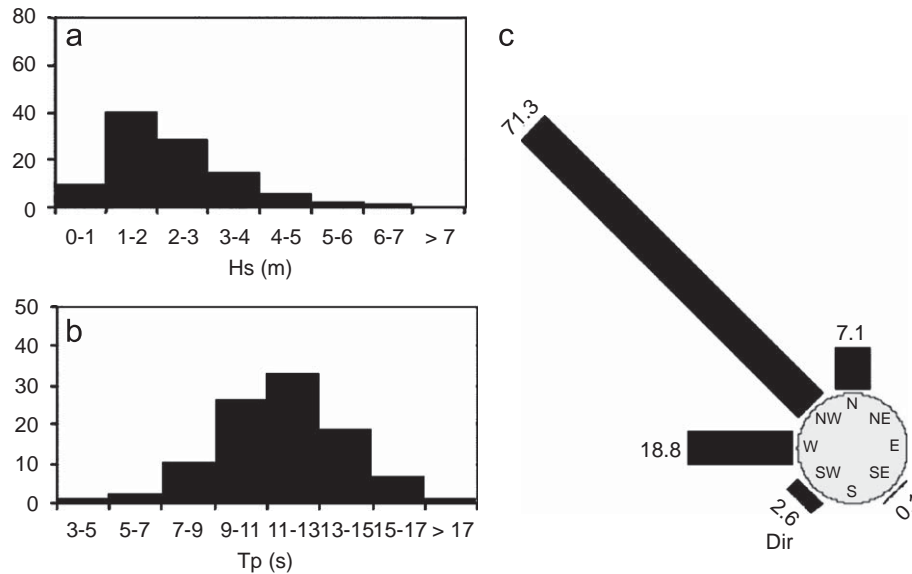


Fig. 2. Typical wave climate in the western Portuguese coast: (a) wave height (Hs, m); (b) wave period (Tp, s); and (c) wave direction (Dir, degrees from North—clockwise) (adapted from Costa et al., 2001).

As within many other shallow coastal systems, friction play an important role in the dynamics of the lagoon; thus, in turn, leads to the establishment of flood dominance. Within this type of asymmetry, the ebb phase lasts longer than the flood phase, resulting in stronger currents during the flood phase (Stanev et al., 2007).

The offshore wave climate 'along the western Portuguese coast (Costa et al., 2001) is characterized commonly by wave heights (Hs) within the range 1–2 m (40% of the records), whilst 22% of the observed values exceed 3 m (Fig. 2). In terms of wave peak periods (Tp), it was observed that 60% of the values were between 9 and 13 s. Wave direction observations showed that 90% of the incoming waves were originating from the West (W) and Norwest (NW) sectors. Waves generate an alongshore southward current (e.g., littoral drift), which promotes the inflow of marine sands into the inlet and resuspend sediments; this affects significantly the hydrodynamic within the lagoon.

2.2. Bathymetric and oceanographic data

The oceanographic data available for this particular study were collected during the "Monitorização Ambiental da Lagoa de Óbidos" Project (MAMBO), a contribution from the Portuguese Hydrographic Institute—IHPT (IHPT, 2001a, b, 2002a, b). The data available included bathymetric surveys, sea-level time-series, currents, wind and wave data.

The project commenced on October 24th, 2000 and lasted for 8 months. The monitoring program incorporated: automatic tidal gauges and current measurements obtained with an Acoustic Doppler Current Profiler (ADCP, RDI WORKHORSE 1200 kHz) inside the Óbidos Lagoon; an ADCP, with module WAVES in the coastal area (RDI WORKHORSE 600 kHz); meteorological automatic station (ANDERAA AWS 2700) and set to collect the bathymetric data with an acoustic sensor. Sea level was measured, between December 2000 and December 2002, at three stations within the lagoon: one located near the inlet (Station B); and two located within the arms (D and E, station locations in Fig. 1). Currents were measured near the inlet (Station A) and along the northern channel (Station B and C) during a tidal cycle on November 26th and 29th, 2000 and July 3rd and 6th, 2001.

In the coastal area, the ADCP (within 20 m water depth) measured the waves from November to December, 2000 and during May 2001.

All of the data were sampled at 10 min intervals, except for the wave height and wind, which were recorded every hour.

2.3. Hydrodynamic model

The numerical model used in this study was MOHID (Martins et al., 2001), a three-dimensional finite volume model. The MOHID hydrodynamic model was used to achieve an accurate characterization of the flow regime in the study area, because it has the ability to simulate flow over complex bathymetry in shallow coastal systems (Vaz et al., 2007). The hydrodynamic equations of MOHID model and the down-scaling methodology have been described by Leitão et al. (2005). Here, we present only the implementation of the Óbidos Lagoon predictive model.

The configuration applied to the Óbidos coastal lagoon included two levels of nested models, with one-way coupling (Fig. 3). To reduce the number of land points in the model area, we rotated the region $\sim 45^\circ$ (see the North indicator, in Fig. 3).

The first level covers the coast between Nazaré and Peniche (between 39.1°N and 39.8°N). The grid spacing is less than 100 m nearshore and approximately 200 m offshore. The total number of grid points is 346 by 250 cells. The model was forced, through prescribed surface elevations from FES95.2 global tidal solution (Le Provost et al., 1998) at the open boundaries in the Northeast, Northwest and Southwest (Fig. 3a). The meteorological data used in the atmospheric forcing was obtained from the MAMBO project automatic station and was concurrent with the simulated period. The meteorological data used were wind speed (ms^{-1}) and direction (degrees from North, clockwise). The time step was 10 s and the horizontal eddy viscosity was $10 \text{ m}^2 \text{ s}^{-1}$. The model was initialized with 'null-free' surface gradients and zero velocities at all of the grid points. A bottom roughness (Manning) coefficient of 0.022 was adopted.

The second level included the Óbidos Lagoon and the transition zone between coastal waters. The total number of grid points is 300 by 340 cells, with a constant grid spacing of about 25 m. The solution of level one was downscaled, to this level. Freshwater

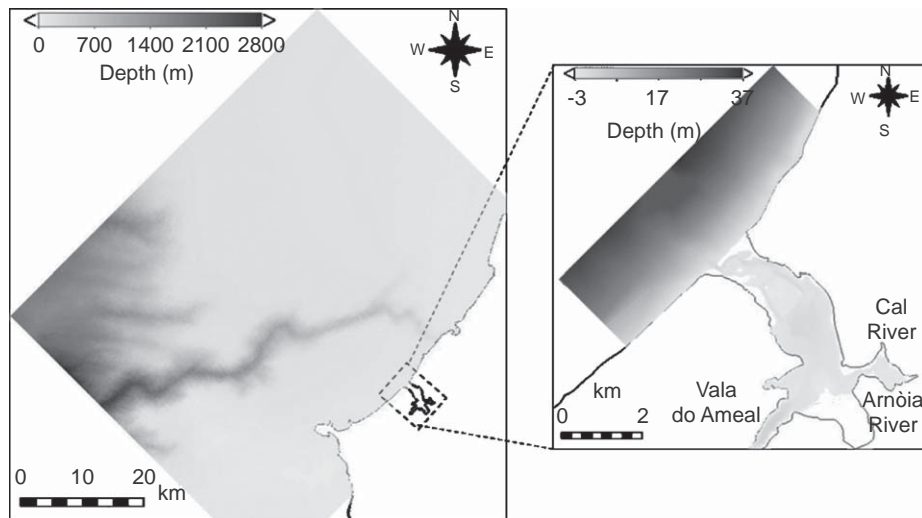


Fig. 3. Domain bathymetry for the two-nested model implemented: (a) Nazaré-Peniche coast and (b) Óbidos Lagoon. The freshwater fluxes are marked in the Óbidos Lagoon domain.

fluxes from river runoff were specified at three locations within the Óbidos Lagoon model, at constant rates for each of the three small rivers: Arnóia, Cal and Vala do Ameal (Fig. 3b). These data, typical of winter and summer months, are described in more detail in Section 2.5. The time step was 5 s and the horizontal eddy viscosity was $2 \text{ m}^2 \text{ s}^{-1}$. A 2D depth-integrated model was used, because it was assumed that the study area presents an homogeneous water column, due to the shallow depths and minor freshwater inputs.

2.4. Wave model

To simulate the wave propagation, the Steady-State Spectral Wave model (STWAVE), developed by the US Army Corps of Engineers (Smith et al., 1998, 2001), was used. STWAVE simulates depth-induced wave refraction and shoaling and it includes additional effects such as current interaction, wave breaking, diffraction (simplified approach), wave-wave interaction and white-capping. The STWAVE model is based upon the assumption that relative phases of the spectral components are random and, thus, phase information, is not tracked (e.g., it is a phase-averaged model).

Wave radiation stresses were calculated with the wave propagation model, which assume the wave's effect over the currents. Since the opposite (current effects over the waves) was not considered, the sea level was simulated assuming 1 m sea-level classes. This meant that for each wave condition, simulations were performed from the hydrographic 0 up to 5 m above the maximum possible tidal level. Afterwards, it was considered acceptable to interpolate wave radiation stresses within the sea-level range of each meter.

The contribution of waves to bed roughness was considered also in the model simulations. For the bottom shear stresses it was considered that total roughness is provided by the sum of the components associated with current and waves. Wave roughness was considered to be the maximum of the $3 \cdot D_{90}$ value (the sieve size for which 90% of the grains by weight are smaller; it provides an estimate of the largest sand grains present in a sample) and an estimation based on the bed forms (ripples and dunes), following the approaches proposed by Van Rijn (1989).

Boundary wave conditions used Hs, Tp and average direction derived from the ADCP (see location, in Fig. 1). To make the number of wave simulations feasible, the wave record was split

into classes of Hs, Tp and direction, using the criteria of approaching: the Hs for the next half meter; the Tp to the closest second; and the direction to the limit of each 25° interval. As such, 27 different offshore wave conditions were adopted. The theoretical JONWASP spectrum was applied at the model boundary. This approach allowed the simulation of a wave sequence, similar to that recorded by the ADCP, using a limited number of wave conditions.

2.5. Simulations

Hydrodynamic simulations were set-up for different physical forcings, representative of distinct situations: (i) tide; (ii) tide and wind; (iii) tide and freshwater river discharges; and (iv) tide and waves. Tidal forcing was considered throughout the model simulations. Others, such as wind, freshwater discharges and waves were used as additional forcing, to highlight the lagoon hydrodynamics. Freshwater flux values are typical of a wet and dry year. The values used for the dry year were 0.1 and $1.6 \text{ m}^3 \text{ s}^{-1}$ for Cal and Arnóia River, respectively; and $0.04 \text{ m}^3 \text{ s}^{-1}$ for Vala do Ameal (Vão, 1991). The values for the wet year were $0.5 \text{ m}^3 \text{ s}^{-1}$ for the Cal River, $5.7 \text{ m}^3 \text{ s}^{-1}$ for the Arnóia River and $0.2 \text{ m}^3 \text{ s}^{-1}$ for Vala do Ameal (Vão, 1991).

The model was run for the time period between November 1st and December 30th, 2000. The first 15 days of results were considered as a 'spin-up' period; these were not included in the results.

3. Results and discussion

The consistency between the simulations and the observations (LSL and currents) were analyzed, at the location of measurements carried out in the Óbidos Lagoon (see Fig. 1, for locations). Results of the inlet-lagoon idealized model were also analyzed, together with numerical model simulations, to provide a better comprehension of the coastal system.

3.1. Lagoon sea level

Fig. 4 depicts the observations and simulations of LSL at Station B (near the inlet), wind data and observed and simulated coastal waves, for the period where the wave height increases slightly.

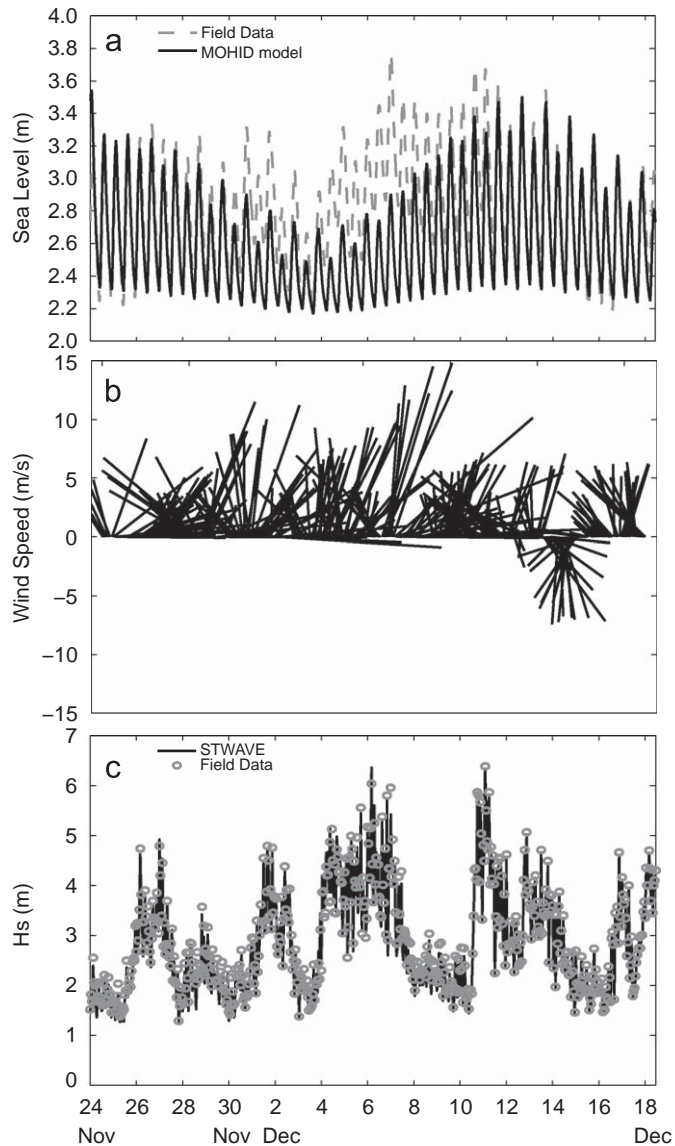


Fig. 4. Comparison between modelled and observed sea-level time-series, at Station B. The simulation period is from November 24th to December 18th, 2000 and includes the forcing due to tide only. Wind data and waves (observations and simulations) are also represented for the same period.

This extends from November 24th, through to December 18th, 2000. The LSL was obtained considering tidal forcing alone (Fig. 4a). The agreement between the simulations and observations is least effective between December 1st and 12th, 2000. During this period, the predicted sea levels do not agree with the measurements because an “abnormal” rise occurs. This behavior is detected also at the other stations inside the lagoon (Station D and E). This is an important result, because it indicates that other relevant physical forcings should be considered, to explain noticeable variations in LSL. Hence, when we analyze the LSL data (a low-pass filter was used to remove the influence of high-frequency processes in measurements), we discovered that tide explains 80% of the variability.

To provide a better idea about how other physical forcing affects the LSL, additional simulations were performed, which introduced forces from wind and freshwater river runoff. Comparisons between these effects and the tidal forcing do not show any significant differences in amplitude. According to other case studies, the sea-level rise caused by river flood occurs only

for discharges above $120 \text{ m}^3 \text{ s}^{-1}$, as observed in the Natsui River, Japan (Nguyen et al., 2007). Here, freshwater fluxes are less than $10 \text{ m}^3 \text{ s}^{-1}$ during a period of heavy rain, whilst average fluxes lie close to $3 \text{ m}^3 \text{ s}^{-1}$.

By observing the wave data and the STWAVE model simulations, it appears that increases in LSL occur often at the same time as a peak in the wave height during a storm, then the sea-level elevation (Fig. 4a and c). The dominant period (wave height values within the range 3–7 m) occurs in the first 10 days of December 2000 and is concurrent with strong winds (of more than 10 ms^{-1} , see Fig. 4b). These intense waves are generated by local winds (sea or wind waves).

To analyze the consistency of these events, we performed comparisons not only for the period of our model simulations, but also for two other periods, including: high wave activity (H_s greater than 3 m) or storm waves (November 28th to December 10th, 2000) and low wave activity (May 11th–23rd, 2001). A correlation was found with wave height and sea-level elevation, during high wave activity periods; no correlation was found for low wave activity. This statement is justified from Fig. 5, which provides simulated and observed LSL for the two periods mentioned above. For both periods, two hydrodynamic model simulations were performed. Wave forcing was not applied in the first simulation (Fig. 5a and b), but it was applied in the second (Fig. 5c and d). Model results from both simulations and wave scenarios show that the model (physic) reproduces the tide and wave forcing, in such a way that simulation and observations agree reasonably well. Not only the general characteristic of the LSL variability is well reproduced by the model, but also the SLR related to wave-induced period, which occurs from November 28th to December 10th, 2000 (Fig. 5c). At the time of SLR occurrence, the wave height is equal to 3 m. Subsequently, SLR increases ($\sim 1 \text{ m}$ in amplitude) together with wave height (reaching 6 m). This kind of response is not observed for low wave activity, because its impact on LSL is negligible (Fig. 5d). This suggests that SLR in the Óbidos Lagoon is influenced by wave motion, such as wave breaking at the entrance, during high wave activity periods. These episodes of storm waves can affect the LSL by about 20%, whereas 1% is affected during low wave activity periods.

The coherence between the two model-sets, in terms of Root Mean Square Error (RMSE), correlation coefficient (r) and model performance (skill), are presented in Table 1. The RMSE errors are discussed as a percentage of the field data mean value.

In general, the highest disagreement was found for tidal forcing during high waves activity, with a RMSE around 36% of the field data mean value. Such an error (RMSE = 1.0 m) might be expected, because tidal forcing includes only the signal of the tide, excluding the wave motion. Minor errors (RMSE = 0.10 m) were obtained when additional wave forcing was included in the model set-up. In this case, the RMSE is $\sim 6\%$. A strong correlation ($r = 0.90$), between model predictions and observed data, was obtained also for tidal and wave forcing, whereas a weaker correlation (0.77) was obtained for tidal forcing. This difference suggests that the model was able to capture well the relative differences between both forcing conditions, demonstrating the importance of waves on the LSL fluctuations. An improved index of agreement (0.94) was found for tidal and wave forcing, which means that the model tends to reproduce, more appropriately, the mean tendency in the field data.

For the period with low wave activity, the disagreement between the computed and observed sea levels, in both cases is small, with the RMSE values lower than 4%. As expected, r was maintained in both cases (0.92). This is evident from the fact that, during low-wave energy fluxes, there are no significance changes in sea-level elevation. The skill index presents a broad interval of

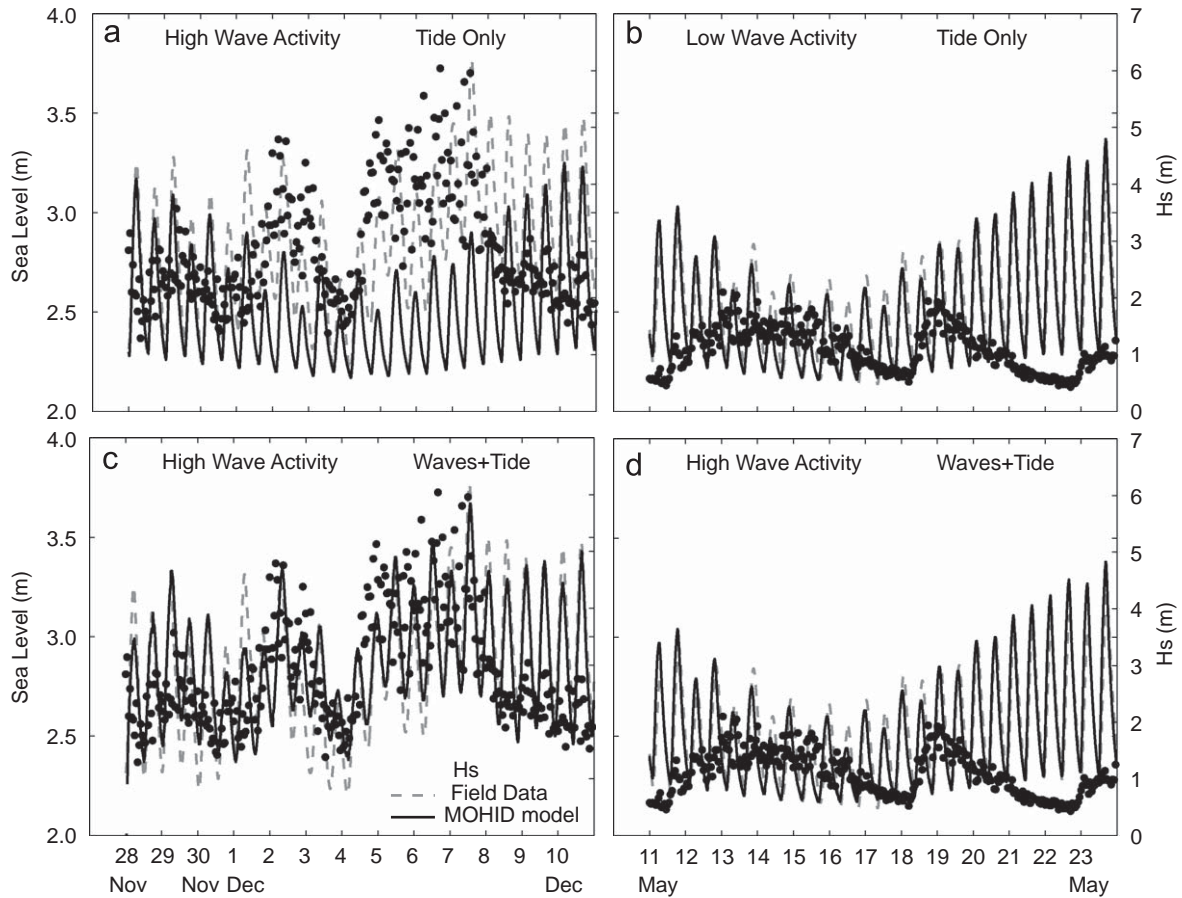


Fig. 5. Lagoon sea level predicted by the model and their comparison with measurements for tidal forcing during high wave (a) and low wave (b) activity periods. The wave-induced forcing for high and low wave activity periods are represented in (c) and (d), respectively. The wave height is represented too.

Table 1

Correlation coefficient, root mean square error and skill between measurements and model predictions, for both simulations: high wave activity and low wave activity.

	High wave activity		Low wave activity	
	Tide	Tide+waves	Tide	Tide+waves
<i>r</i>	0.77	0.90	0.92	0.92
RMSE (m)	1.0	0.10	0.15	0.15
Skill	0.68	0.94	0.99	0.90

0.90–0.99 (within perfect agreement yielding a skill of 1.0), indicating that the model shows good accuracy.

It may be concluded that the dominant forcing on the hydrodynamic features of the Óbidos Lagoon is tidal forcing. However, to obtain a more realistic representation of the system, it is important to include the wave motion, coupled to the tidal signal.

3.2. Ocean sea level

The sea level inside the coastal lagoon was analyzed through various physical forcings and quantitative approaches, to understand the variability introduced by storm waves, during certain periods. However, it is important to understand if the same variability occurs in the ocean sea level (OSL). Fig. 6a, b presents the OSL and the LSL at Station B (lower lagoon) and Station E

(upper lagoon), which extends from December 3rd to 10th, 2000 (high wave activity) and from May 14th to 21th, 2001 (low wave activity), respectively. The wave energy flux (E_f) derived from the Hs, Tp and wave direction data, is also shown. As shown by the data, LSL with wave forcing (period of high wave activity) is above that of the ocean recorder (see Fig. 6a). The same behavior was not related by the data provided during low wave activity periods, which shows the LSL at the same level as the OSL (Fig. 6b). This behavior reveals that LSL increases with increasing E_f and is higher than the OSL. It appears that E_f is responsible for the LSL rise (Fig. 6a). A similar behavior was observed in Manihiki and Rakahanga atolls of the Cook Islands in South Pacific Ocean, where the average of the LSL increases significantly during large wave periods (Callaghan et al., 2006).

It has been shown that LSL is above the OSL for certain wave periods, but there are some questions to be answered. The following section provides a simplified inlet-lagoon idealized model, to understand the major dynamic controls on the coastal system.

3.3. Simplified inlet-lagoon model

Numerical models are complex and involve long computation calculus, because they deal with many variables and parameterizations. For this reason, relatively simple analytical expressions of an inlet-lagoon idealized model were derived to understand the role of the wave radiation stresses in the super-elevation, or wave set-up, of the LSL. A simple inlet-lagoon idealized model, based

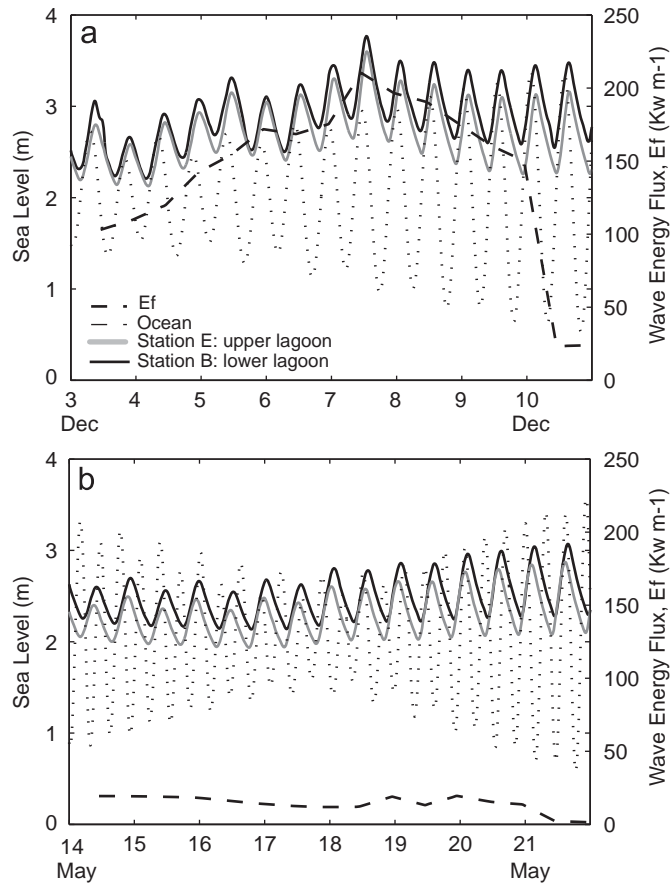


Fig. 6. Measured ocean and lagoon sea levels at Station B (lower lagoon) and Station E (upper lagoon), from December 3rd to 10th, 2000 (a) and May 14th to 10th, 2001 (b). Averaged wave energy flux derived from wave data (wave height, period and direction) is presented also.

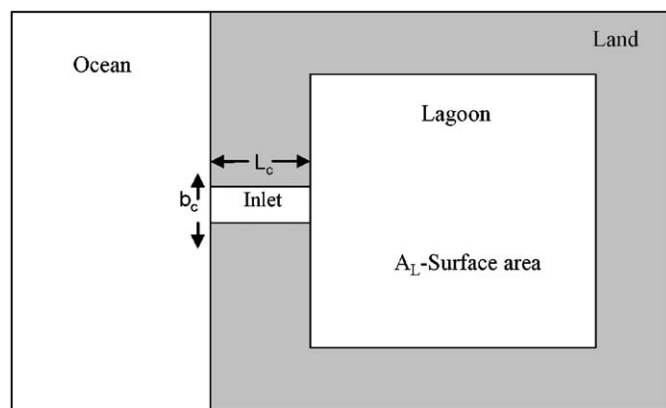


Fig. 7. Schematic representation of the inlet-lagoon system.

upon mathematical expressions is prescribed considering the configuration depicted in Fig. 7. A simple inlet-lagoon model is now developed, implemented easily on a spread sheet, to predict the lagoon dynamics under different physical forcings.

The simple inlet-lagoon model can be described by the following system of equations. Considering conservation of water volume for the system, when assuming the lagoon fluctuations uniformly over its horizontal area, the LSL can be expressed by

$$\eta_L(t + \Delta t) = \eta_L(t) + \Delta t \frac{Q_c(t + \Delta t)}{A_L} \quad (1)$$

where A_L and η_L are the area and the sea level of the lagoon, respectively (the index “L” stands for “lagoon”), t is the time, Δt is the time step and Q_c is the total rate of inflow at the inlet (or channel, “c” stands for “channel”). The evolution of inlet flow is presented in the form of Eq. (2), which is based upon a transport equation that considers the pressure gradient, bottom friction and wave radiation stresses.

$$Q_c(t + \Delta t) = Q_c(t) + \Delta t \left(g \frac{\eta_o - \eta_L}{L_c} A_c(t) - C_d \frac{|Q_c(t)| Q_c(t)}{A_c(t)^2} b_c + R_S b_c \right) \quad (2)$$

where η_o is the ocean sea level, A_c , L_c and b_c the cross-sectional area of the inlet and its length and width, R_S is the radiation stresses along the waves and C_d is the drag coefficient. The OSL is prescribed as

$$\eta_o = a \cos(\omega t) \quad (3)$$

where a is the tidal amplitude and ω is the tidal angular frequency. The drag coefficient is given by a Manning formula (Chow, 1973),

$$C_d = g n^2 h_c^{-1/3} \quad (4)$$

where g is the acceleration due to gravity ($g \sim 10 \text{ ms}^{-2}$), n is the Manning coefficient and h_c is the inlet depth. The cross-sectional area of the inlet is given by

$$A_c(t) = b_c \left(h_c + \frac{\eta_L + \eta_o}{2} \right) \quad (5)$$

where b_c and h_c is the inlet width and depth, respectively, η_o is the ocean sea level and η_L is the sea level in the lagoon.

To investigate the effect of wave radiation stresses on the SLR, an inlet-lagoon-simplified model of the Óbidos Lagoon was applied. This adopted a lagoon horizontal area of about $7.0 \times 10^6 \text{ m}^2$, an inlet of 100 m in length, 1 m depth and 25 m width. The value of R_S ($0.10 \text{ m}^2 \text{ s}^{-2}$) was obtained through the STWAVE model. This value was calculated based upon the linear wave theory for shallow water-waves (Smith et al., 2001). The data provided for the model calculations were H_s , T_p and direction. The results are shown in Fig. 8a, for two cases, with and without R_S forcing. This distinction is important because, under the two different situations, the physical balances differ substantially. The dark gray curve shown in Fig. 8a demonstrates super-elevation in the LSL above the OSL (black-dashed curve), in the case of the R_S . The impact of wave radiation stresses on sea level in the lagoon is controlled by wave pumping inflow in the inlet. As a result, an increase in the LSL occurs above the OSL. This means that the sea level increases to maintain the pressure gradient and friction equilibrium.

At this phase, it is clear that wave radiation stresses are relevant to the pumping of water inside the lagoon; however, what is the role of the inlet? If an inlet cross-sectional area is assumed which is that double of the real inlet and the channel ($1.2 \times 10^4 \text{ m}$ length, 30 m depth and 2000 m width) of the Tagus Estuary (the largest estuary in Portugal, located near Lisbon), we obtain the light gray curve and the dark curve shown in Fig. 8b, respectively. In this case, the super-elevation in the lagoon tends to diminish and within the estuary, the sea level remains over that of the ocean curve (black-dashed). This kind of response is due to the fact that the export of water through the inlet depends upon the relationship between the capacity of the cross-sectional inlet area (A_c) and the volume of the lagoon ($A_L \times h_L$). This difference is well illustrated when comparing the Tagus Estuary, mean volume $\sim 3 \times 10^9 \text{ m}^3$ and the cross-sectional channel area $\sim 6 \times 10^4 \text{ m}^2$, with the lagoon mean volume $\sim 1.4 \times 10^7 \text{ m}^3$ and the inlet area $\sim 25 \text{ m}^2$. Similar conclusions were reached by Stanev et al. (2003a), in terms of the response of tidal basins to ocean forcing.

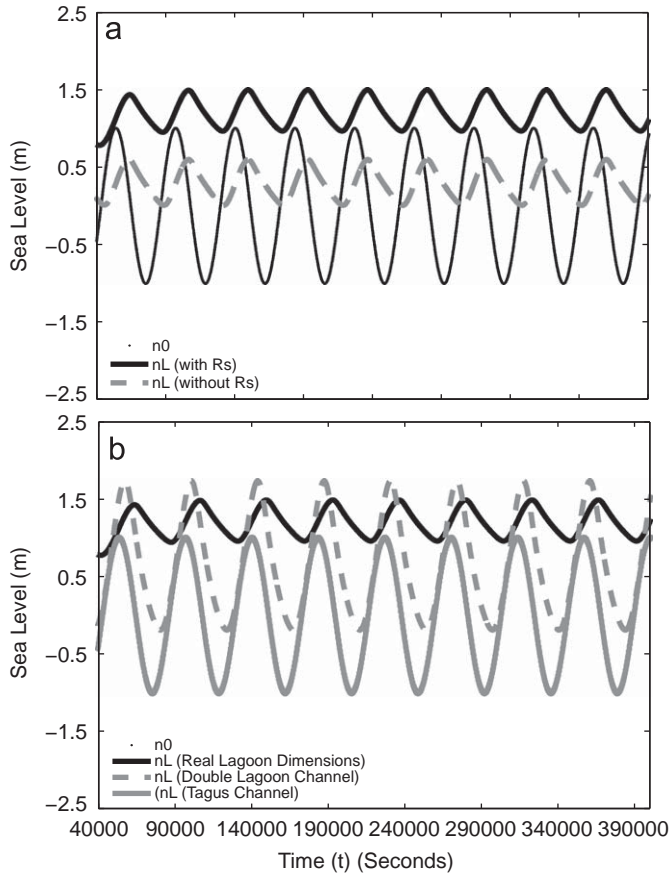


Fig. 8. Lagoon and ocean sea level predicted using the simplified inlet-lagoon model, for the case with and without waves forcing (a); and with waves forcing for different channel cases: real lagoon dimensions, a channel with double of dimensions of the real one and the Tagus estuary channel (b).

It has demonstrated that the import and export of water through the inlet depends upon the ratio between the maximum storage capacity of the basin and the amount of water permanently stored within it. In fact, the adjustment of the sea surface in the bay, to oscillations in the open sea is controlled by the ratio between the cross-sectional area of the inlet and the area of the bay.

3.3.1. Analytical solution

The idealized model described here is similar to that prescribed for the narrow tidal inlets of the East Frisian Wadden Sea, adding the effect of wave radiation stresses. Our simplified inlet-lagoon model indicates that the dominant balance is between waves, pressure forces and friction (Eq. (6)). In comparison, according to the idealized model described by Stanev et al. (2003a), the major response is between the pressure forces and friction. In addition, Stanev et al. (2003b) also considered the channel area (A_c), constant over time and a linear friction dissipation term. These simplifications were introduced, by the authors, to derive an analytical solution to the inlet-lagoon model. In the present study, an analytical solution of Eq. (9) is proposed, which includes the effect due to wave radiation stresses.

$$\frac{dQ}{dt} = g \frac{\eta_o - \eta_L}{L_c} A_{c_{mean}} - C_d \frac{|u_{mean}|}{h_c} Q_c(t) + R_S b_c \quad (6)$$

Assuming ω_H^2 as the pumping frequency given by

$$\omega_H^2 = \frac{g A_{c_{mean}}}{L_c A_L} \quad (7)$$

and the differential form of Eq. (1) is

$$\frac{d\eta_L}{dt} = \frac{Q_c(t)}{A_L} \quad (8)$$

From Eqs. (6) and (8) we obtained the mathematically continuous form of Eq. (2)

$$\frac{d^2 \eta_L}{dt^2} + \delta \frac{d\eta_L}{dt} + \omega_H^2 \eta_L = \omega_o^2 \eta_o + \frac{R_S b_c}{A_L} \quad (9)$$

The bottom friction parameterization was obtained from Eq. (4)

$$\delta = C_d \frac{|u_{mean}|}{h_c} = \frac{g n^2}{h_c^{4/3}} |u_{mean}| \quad (10)$$

In Stanev et al. (2003b) an analytical solution of Eq. (9) was presented, assuming the following solution for the ocean sea level:

$$\eta_o = a \cos(\omega t), \quad \omega = \frac{2\pi}{T} \quad (11)$$

In fact, Eq. (9) is the classical damped, driven harmonic oscillator, whose class of analytical solutions is well known. The damping term is parameterized by Eq. (10). The intrinsic oscillation frequency, characterized solely by the lagoon geometry, is parameterized by Eq. (7), whilst the driving frequency, which represents ocean forcing, is parameterized by Eq. (11). The damped, driven harmonic oscillator is characterized over time, by two regimes: a transient regime, where the intrinsic part of the solution is calculated by solving the homogeneous form of Eq. (9), coexists with the driving part of the solution, where both characteristic frequencies (ω_H and ω) play a role in the level motion; and a driven regime, where the intrinsic part of the solution is completely damped by the system, and where the sole remaining characteristic frequency is ω , affected only by a phase and amplitude shift. The transient regime occurs at the “turn on” of the harmonic oscillator and is eventually dissipated. It is assumed that the system is permanently in the purely driven regime. This assumption has the benefit of discarding the task of considering the solutions for the homogeneous equation. Hence, only a particular, non-trivial solution of Eq. (9) needs to be considered, to predict the sea level in the lagoon. The particular solution of Eq. (9) can be described by

$$\eta_L(t) = \alpha a \cos(\omega t - \theta) + \frac{R_S b_c}{A_L \omega_H^2} \quad (12)$$

where α is the attenuation of ocean tidal wave inside the lagoon

$$\alpha = \sqrt{\frac{\omega_H^4}{(\omega_H^2 - \omega^2)^2 + \delta^2 \omega^2}} \quad (13)$$

and θ is the phase delay associated with the lagoon inlet

$$\theta = \arctan\left(\frac{\delta \omega}{\omega_H^2 - \omega^2}\right) \quad (14)$$

the solution can be simplified in the follow equation

$$\eta_L(t) = \alpha a \cos(\omega t - \theta) + \frac{R_S L_c}{g H_c} \quad (15)$$

This solution is similar to that presented by Stanev et al. (2003b), with a difference in the second term of the right-hand side of equation-wave radiation stress forcing. Note how the intrinsic frequency of the system (ω_H) only affects a shift in the amplitude (Eq. (13)) and phase (Eq. (14)) of the ocean driven system Eq. (15). The harmonic oscillator is a simplified model of the lagoon and is adequate, in the sense that it represents the nature of the flushing tide and waves.

Based upon the linear solution of Eq. (15), it is possible to estimate the sea-level elevation (second term on the right-hand side of the equation), due to the gradient of radiation stresses. In the Óbidos Lagoon case study, the sea-level elevation due to sea waves over the inlet is of the order 1 m (considering the same values referred to in the previous Section); this is confirmed by the observations and numerical model outputs (2D primitive equation and simplified model). The term associated with the wave's effect (or any other shear stress aligned with the channel, e.g., wind) shows that the longer the inlet or channel, the more intense is the difference between OSL and LSL. In other words, the sea-level gradient is proportional to R_S ; this means that, for the same gradient, the difference between the ocean and the lagoon sea level increases with L_c . The term also shows that the difference in sea level decreases with increasing channel depth, for the same shear stress.

Only sea waves can introduce a shear stress which, in turn, induces a significant sea-level gradient between the ocean and the lagoon. The wind stress (Eq. (16), ρ_w is the water density) can be considered also as a forcing term in the solution of Eq. (16). An extreme wind of 100 kmh^{-1} , aligned with the inlet direction, corresponds approximately to a shear stress of $0.001 \text{ m}^2 \text{ s}^{-2}$. Thus, it corresponds to an increase of only 1 cm in sea level, in the case of the Óbidos Lagoon.

$$\eta_L(t) = \alpha a \cos(\omega t - \theta) + (R_S + (\tau_{wind}/\rho_w)) \frac{L_c}{gH_c} \quad (16)$$

Fig. 9a, b compares the results obtained with the analytical model, using the results of the simplified inlet-lagoon idealized model. The analytical model is able to reproduce the main

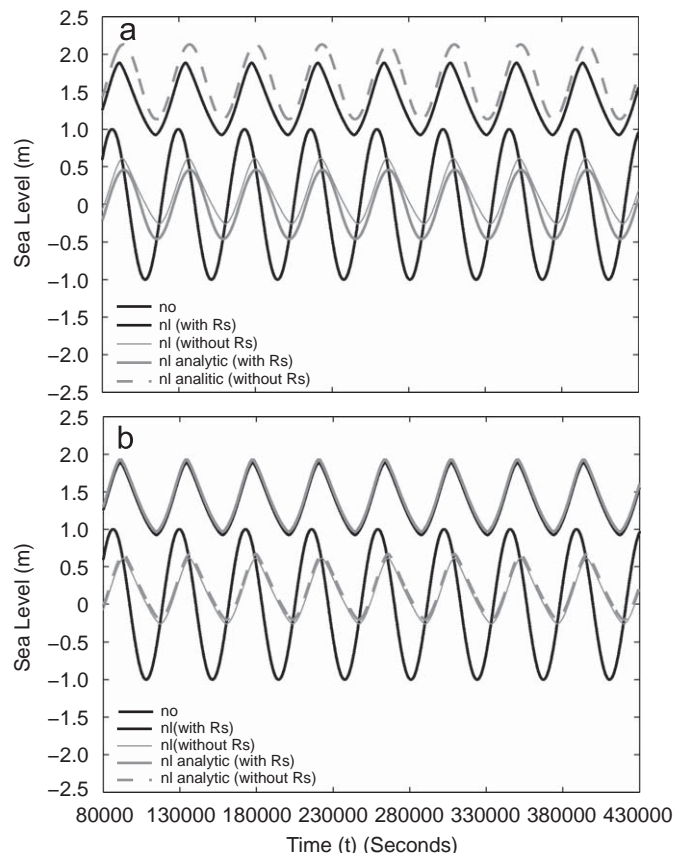


Fig. 9. Comparison between analytical solution and simplified model results, with and without wave forcing, considering a cross-sectional channel area variable in time (a) and assuming a constant cross-section channel area (b).

differences between OSL and LSL. It is also able to reproduce the effect of a constant shear stress associated with sea waves over the inlet. However, the simplifications introduced to obtain the analytical solution generate some differences. The most important is the disappearance of the tidally driven residual difference, between ocean and LSL. This residual difference, present in the real data, is of the order 20 cm, between the ocean and the lower station in the lagoon (Fig. 6b). A similar difference can be observed in the simplified model results, without the effect of waves (see Fig. 9a). When the cross-sectional channel area is considered constant over time and equal to $A_{c,mean}$ in the idealized model, the difference between OSL and LSL disappears; and only minor amplitude and phase differences are maintained. This is due to the fact that the friction term in the analytical solution is linear and; if it is assumed to be linear in solutions (numerical and analytical), then they match (Fig. 9b). The simplified model assumes a variable cross-sectional channel area over time and, considering a null drag coefficient, the residual gradient would disappear. On the other hand, if the drag coefficient is not considered as being null, the residual gradient will appear in the results.

These result shows that the residual gradient is generated by tidal asymmetry associated with the non-linear terms present in the simplified model: friction ($C_d|u_c|u_c/H_c$) and mass conservation ($d\eta_L/dt = u_c A_c/A_L$).

3.4. Current velocities

Fig. 10 shows the measured and simulated time-series of current velocity near the inlet (Station A) and along the channel (Station B) for November 29th, 2000. The LSL at Station B is also shown; this is the only station with available current and sea-level data. The variability in the surface currents (Fig. 10a and b) is well reproduced by the model, revealing stronger currents near the inlet and weaker along the channel. However, in spite of the high skill score (0.80 and 0.85), the model results underestimate the observations. The simulated currents also reveal semi-diurnal variations.

Another interesting feature captured by the model is the agreement between the tidal asymmetry and the current velocity, at Station B (Fig. 10b and c). As shown by observations and simulations, the lagoon is flood-dominated, with the duration of the ebb phase ($\sim 7 \text{ h}$) being longer than that of the flood phase (5 h). This tidal asymmetry results in stronger currents ($\sim 1.0 \text{ ms}^{-1}$) during the flood phase, whilst weaker currents ($\sim 0.5 \text{ ms}^{-1}$) during the ebb phase.

The spatial patterns of currents in the lower lagoon, for tidal forcing and tide-wave forcing, are presented in Fig. 11. The upper lagoon was not presented because there are no significant differences between phases (ebb and flood) and the physical forcings (tide and waves). The times of the flood and the ebb, for tidal and wave forcing, can be seen in Fig. 11a and b, respectively. Predictions with no wave forcing are presented in Fig. 11c and d for flood and ebb phases, respectively. The timing chosen to analyze the currents patterns reflects the case of the time that corresponds to the current maximum. The major difference between the simulations is the presence of the alongshore current, revealing that the model is able to reproduce the wave motion when forcing is supplied by waves. In terms of magnitudes there are no significant differences between the simulations. As shown by the simulated time-series, the spatial pattern also reveals a flood phase characterized by stronger velocities. Regarding the main hydrodynamics features of the study area, the forcing due to tide and waves is more realistic, than forcing with only by the tide.

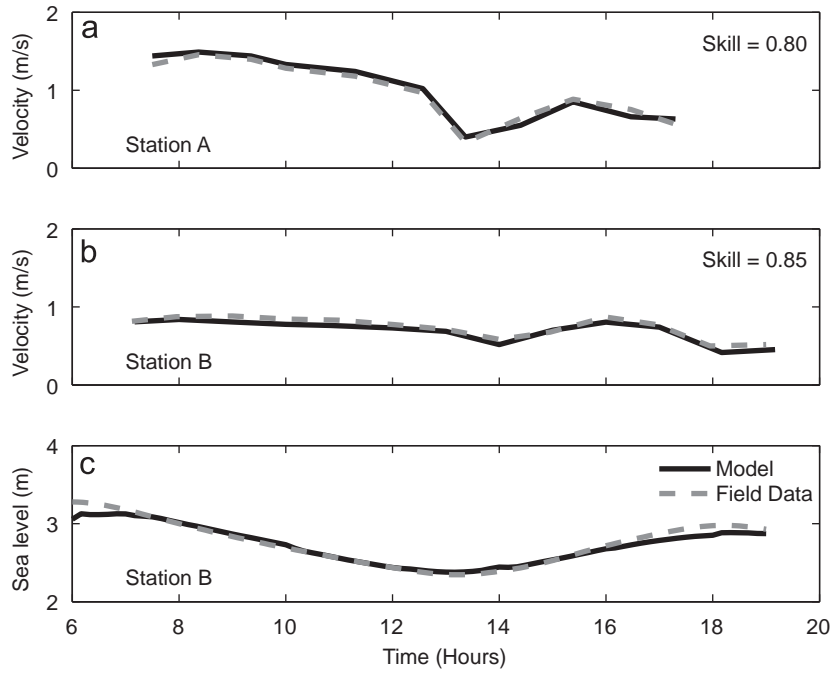


Fig. 10. Measured and simulated time-series of current velocity, near the inlet (Station A, a) and along the channel (Station B, b) for the 29th November 2000. The lagoon sea level at Station B is also shown (c).

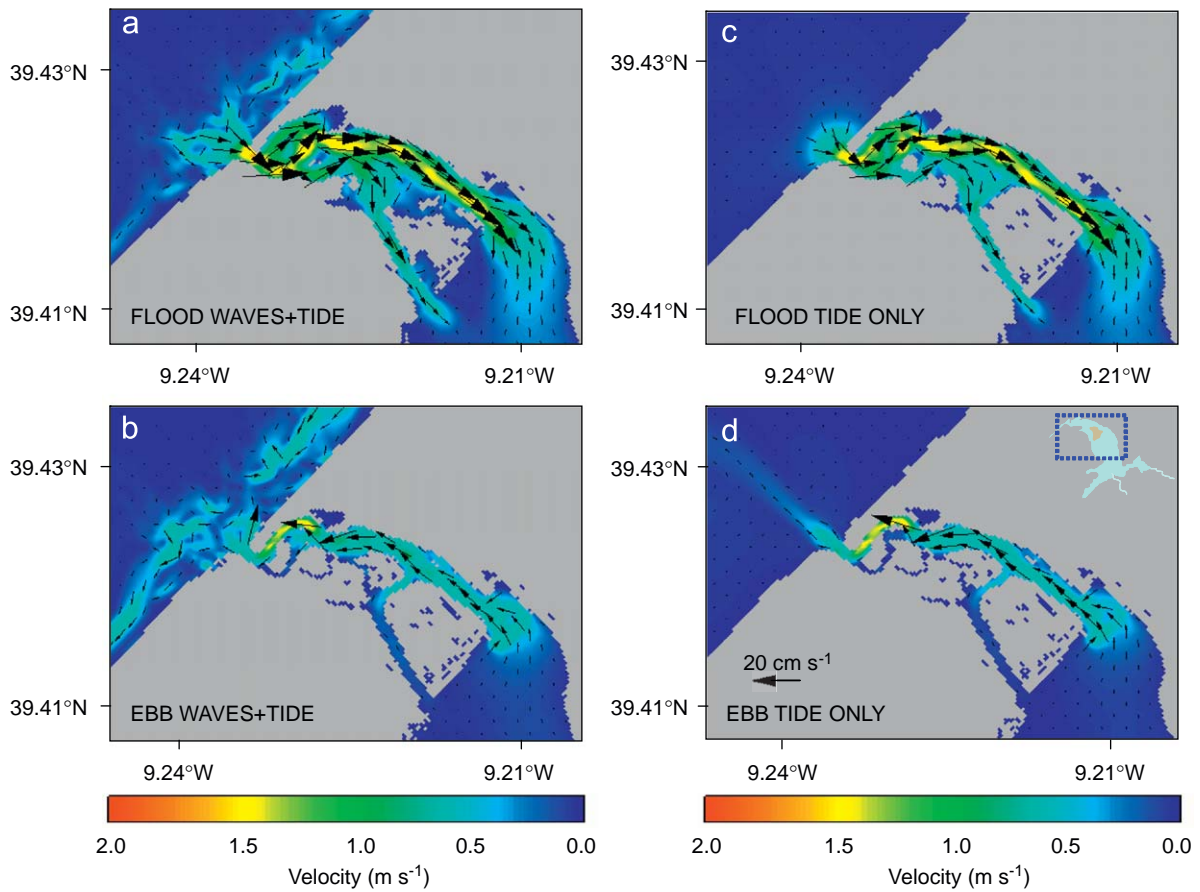


Fig. 11. Spatial patterns of currents in the lower lagoon, for tidal and wave forcing at the times of flood (a) and ebb (b). The times of flood and ebb for tidal forcing are represented in (c) and (d), respectively.

4. Conclusions

Sea-level variations in the Óbidos Lagoon are related to tidal forcing, as well as wave-induced forces. Good model predictions were obtained for the lagoon tidal amplitude, under different physical forcings. The model shows an ability to reproduce the observed temporal variability in the LSL and current velocities, presenting skill coefficients of higher than 0.68.

Field measurements and model predictions show that sea-level elevation in the lagoon is above the OSL during high wave activity periods. In addition, the simplified inlet-lagoon idealized model provides a good understanding of the wave pumping inflow, showing the importance of wave radiation stresses in the super-elevation. Dynamically, this could have two explanations: (1) wave set-up or radiation stress, due to waves; and (2) the tidal inlet morphology. Wave set-up height depends not only upon offshore wave height but also on tidal inlet morphology (mainly depth and length). The deeper and shorter is the morphology, more the wave set-up is reduced, as shown by the numerical solution of the simple idealized model.

Acknowledgements

This work was carried out with the financial support of Águas do Oeste S.A (AdO), as part of the project “Monitoring and modelling the Óbidos Lagoon and Foz do Arelho submarine outfall”. In July 2004, AdO initiated the supervision of a Monitoring Program in the Óbidos Lagoon and coastal area, with the support of Instituto Superior Técnico (IST) from the Universidade Técnica de Lisboa (IST) and Instituto de Investigação das Pescas e do Mar (IPIMAR).

The authors also wish to thank to Nuno Vaz from Aveiro University working in MARETEC/IST at this time, for suggestions and incentive provided during this work.

References

- Angwenyi, C.M., Rydberg, L., 2005. Wave-driven circulation across the coral reef at bamburi Lagoon, Kenya. *Estuarine, Coastal and Shelf Science* 63, 447–454.
- Callaghan, D.P., Nielsen, P., Cartwright, N., Gourlay, M.R., Baldock, E.T., 2006. Atoll lagoon flushing forced by waves. *Coastal Engineering* 53, 691–704.
- Carvalho, S., Moura, A., Gaspar, M.B., Pereira, P., Fonseca, L.C., Falcão, M., Drago, T., Leitão, F., Regala, J., 2005. Spatial and inter-annual variability of the macrobenthic communities within a coastal lagoon (Óbidos Lagoon) and its relationship with environmental parameters. *Acta Oecologica* 27, 143–159.
- Carvalho, S., Gaspar, M.B., Moura, A., Vale, C., Antunes, P., Gil, O., Fonseca, L.C., Falcão, M., 2006. The use of the marine biotic index AMBI in the assessment of the ecological status of the Óbidos Lagoon (Portugal). *Marine Pollution Bulletin* 52, 1414–1424.
- Chow, 1973. *Open-Channel Hydraulics*. McGraw-Hill International Editions. Civil Engineering Series. 1973. ISBN 0.07-Y85906-X.
- Costa, M., Silva, R., Vitorino, J., 2001. Contribuição para o estudo do clima de agitação marítima na costa Portuguesa. *2as Jornadas Portuguesas de Engenharia Costeira e Portuária*. Sines, Outubro de 2001 (in Portuguese).
- Dunn, S.L., Nielsen, P., Nielsen, Madsen, A.P., Evans, P., 2000. Wave setup in Rivers. *ASCE International Conference on Coastal Engineering*, Sydney, Australia, pp. 3432–3445.
- Dunn, S.L., 2001. Wave setup in River entrances. Doctor Thesis in Department of Civil Engineering, University of Queensland. Brisbane, Australia, 191p, published.
- Fortunato, A.B., Oliveira, A., 2007. Case study: promoting the stability of the Óbidos Lagoon inlet. *Journal of Hydraulic Engineering* 133 (7), 816–827.
- Guza, R.T., Thornton, E.B., 1981. Wave set-up on a natural beach. *Journal of Geophysical Research* 86 (C5), 4133–4137.
- Hanslow, D.J., Nielsen, P., 1992. Wave setup on beaches and in River entrances. In: *Proceedings of 23rd International Conference on Coastal Engineering*, pp. 240–252.
- Hanslow, D.J., Nielsen, P., Hibbert, K., 1996. Wave setup in River entrance. In: *Proceedings of 25th International Conference on Coastal Engineering*, pp. 2244–2257.
- IHPT, 2001a. *Monitorização Ambiental da Lagoa de Óbidos NOV 2000–JUN 2001*. Relatório Técnico Final, Report TF. 08/ 2001 (in Portuguese).
- IHPT, 2001b. *Monitorização Ambiental da Lagoa de Óbidos JUL 2001–DEZ 2001*. Relatório Técnico Final, Report PT. OC. 06/2001 (in Portuguese).
- IHPT, 2002a. *Monitorização Ambiental da Lagoa de Óbidos DEZ 2001–ABR 2002*. Relatório Técnico Final, Report PT. OC. 02/2002 (in Portuguese).
- IHPT, 2002b. *Monitorização Ambiental da Lagoa de Óbidos MAI 2002–AGO 2002*. Relatório Técnico Final, Report PT. OC. 05/2002 (in Portuguese).
- Leitão, P., Coelho, H., Santos, A., Neves, R., 2005. Modelling the main features of the Algarve coastal circulation during July 2004: a downscaling approach. *Journal of Atmospheric and Oceanic Technology* 10 (4), 1–42.
- Le Provost, C., Lyard, F., Molines, J.M., Genco, M.L., Rabilloud, F., 1998. A hydrodynamic ocean tide model improved by assimilating a satellite altimeter derived data set. *Journal of Geophysical Research—Oceans* 103, 5513–5529.
- Longuet-Higgins, M.S., Stewart, R.W., 1960. Changes in the form of short gravity waves on long waves and tidal currents. *Journal of Fluid Mechanics* 8, 565–583.
- Longuet-Higgins, M.S., Stewart, R.W., 1962. Radiation stress and mass transport in gravity waves with application to surf beat. *Journal of Fluid Mechanics* 13, 481–504.
- Longuet-Higgins, M.S., Stewart, R.W., 1964. Radiation stress in water waves; a physical discussion with application. *Deep Sea Research* 11, 529–540.
- Longuet-Higgins, M.S., Stewart, R.W., 1973. The mechanics of the surf zone. In: *Proceedings of the 13th International Congress on Theoretical and Applied Mechanics*. Springer, Berlin, pp. 213–228.
- Malhadas, S.M., 2008. *Modelação do impacto de emissários submarinos em zonas costeiras-caso da Foz do Arelho*. Msc. Thesis for the Msc. degree in environmental engineering. Instituto Superior Técnico, Universidade Técnica de Lisboa, Lisboa, Portugal, 95 p., published (in Portuguese).
- Martins, F., Leitão, P.C., Silva, A., Neves, R., 2001. 3D modelling in the Sado estuary using a new generic vertical discretization approach. *Oceanologica Acta* 24 (1), 551–562.
- Nielsen, C., Apelt, C., 2003. The application of wave induced forces to two-dimensional finite element long wave hydrodynamic model. *Ocean Engineering* 30, 1233–1251.
- Nguyen, X., Tanaka, H., Nagabayashi, H., 2007. Wave setup at River and Inlet Entrances Due to an Extreme Event. To appear in *Proceedings of International Conference on Violent Flows*, Organized by RIAM, Kyushu University, Fukuoka, Japan.
- Oliveira, A., Fortunato, A.B., Rego, J.R.L., 2006. Effect of morphological changes on the hydrodynamics and flushing properties of the Óbidos Lagoon (Portugal). *Continental Shelf Research* 26, 917–942.
- Oshiyama, S., Lee, H., Tanaka, H., 2001. Fluctuation characteristics of water level in medium-and-small scale River mouths. In: *Proceedings of 25th International Conference on Coastal Engineering*, JSCE, Vol. 48, pp. 411–415 (in Japanese).
- Rego, J., 2004. *Hidrodinâmica da Lagoa de Óbidos*. B.Sc. Thesis for the B.Sc. degree in Geophysical Sciences—Oceanography, Faculdade de Ciências da Universidade de Lisboa, published (in Portuguese).
- Santos, M., Neves, R., Leitão, P.C., Pereira, P., Pablo, H., Fernandes, L. D., Carvalho, S., Alves, C., 2006. Qualidade da água da lagoa de Óbidos: Que futuro? In: *Proceedings of 12º Encontro nacional de Saneamento Básico*, 24–27 Outubro, Cascais. ISBN:978-972-95302-8-9.
- Smith, J. M., Militello, A., Smith, S. J., 1998. Modeling waves at Ponce de Leon Inlet, Florida. In: *Proceedings of 5th International Workshop on Wave Hindcasting and Forecasting*, Environment Canada, Downsview, Ontario, pp. 201–214.
- Smith, J. M., Sherlock, A.R., Resio, D.T., 2001. STWAVE: Steady-state wave model user's manual for STWAVE, Version 3.0. ERDC/CHL SR-01-1, US Army Engineer Research and Development Center, Vicksburg, MS <<http://chl.wes.army.mil/research/wave/wavesprg/numeric/wttransformation/download/erdc-chl-sr-01-11.pdf>>.
- Stanev, E.V., Wolff, J.O., Burchard, H., Bolding, K., Floser, G., 2003a. On the circulation in the East Frisian Wadden Sea: numerical modeling and data analysis. *Ocean Dynamics* 53, 27–51.
- Stanev, E.V., Floser, G., Wolff, J.O., 2003b. First- and higher-order dynamical controls on water exchanges between tidal basins and the open ocean. A case study for the East Frisian Wadden Sea. *Ocean Dynamics* 53, 146–165.
- Stanev, E.V., Flemming, B.W., Bartholoma, A., Staneva, J., Wolff, J.O., 2007. Vertical circulation in shallow tidal inlets and back-barrier basins. *Continental Shelf Research* 27, 798–831.
- Tanaka, H., Nagabayashi, H., Yamauchi, K., 2000. Observations of wave set-up height in a River mouth. In: *Proceedings of 27th International Conference on Coastal Engineering*, pp. 3458–3471.
- Tanaka, H., Lee, H.S., Furumichi, K., 2003. Influence of morphological change on water level rise at the Shiribetsu River mouth. *Journal of Hydroscience and Hydraulic Engineering* 21 (1), 71–78.
- Troussellier, M. (Lead Author) and Gattuso, J. P., (Topic Editor), 2007. *Coastal Lagoons*. In: *Encyclopedia of Earth*. Eds. Cutler J. Cleveland (Washington, D.C.: Environmental Information Coalition, National Council for Science and the Environment). (First published in the *Encyclopedia of Earth* 21.11.2006; last revised 13.08.2007; retrieved 15.11.2007). <http://www.eoearth.org/article/Coastal_lagoon>.
- Van Rijn, L.C., 1989. *Sediment Transport by Currents and Waves Handbook*. Delft Hydraulics, Report H 461 p.
- Vão-Arquitectos Associados, 1991. *Estudo de Recuperação e Ordenamento da Lagoa de Óbidos, Concha de São Martinho do Porto e Orla Litoral Intermédia*. Vols. I, II and V (in Portuguese).
- Vaz, N., Dias, J.M., Leitão, P.C., Nolasco, R., 2007. Application of the MOHID-2D model to a mesotidal temperate coastal lagoon. *Computers & Geosciences* 28, 1204–1209.